

The environmental envelope of fires in the Colombian Caribbean



N. Hoyos^{a,*}, A. Correa-Metrio^b, A. Sisa^c, M.A. Ramos-Fabiel^d, J.M. Espinosa^a,
J.C. Restrepo^e, J. Escobar^{c,f}

^a Departamento de Historia y Ciencias Sociales, Universidad del Norte, Barranquilla, Colombia

^b Instituto de Geología, Universidad Nacional Autónoma de México, Ciudad de México, Mexico

^c Departamento de Ingeniería Civil y Ambiental, Universidad del Norte, Barranquilla, Colombia

^d Posgrado en Ciencias Biológicas, Universidad Nacional Autónoma de México, Ciudad de México, Mexico

^e Departamento de Física y Geociencias, Universidad del Norte, Barranquilla, Colombia

^f Smithsonian Tropical Research Institute, Ciudad de Panamá, Panamá

ARTICLE INFO

Article history:

Received 25 November 2016

Received in revised form

5 May 2017

Accepted 6 May 2017

Keywords:

Fire

MODIS

Colombia

Caribbean

ABSTRACT

Fire is an important disturbance agent for terrestrial ecosystems, particularly in tropical and subtropical regions where its occurrence is controlled by multiple biophysical and anthropogenic variables. We assessed the temporal and spatial patterns of active fire detections (MODIS product MCD14ML) in the Caribbean region of Colombia between 2003 and 2015, using time series, cross-correlation, hot spot and density techniques. We also assessed the environmental envelope of active fires by evaluating the effect of multiple biophysical and anthropogenic variables on fire presence/absence using generalized linear models (GLMs). Results show that fires follow a clear intra-annual cycle, with 86% of fire events taking place during the region's main dry season (December–March). There is also inter-annual variability related to the Tropical North Atlantic (TNA) quasi-decadal climatic oscillation. Active fires exhibit a distinctive spatial pattern, with regional hotspots. The set of variables that best explain fire presence/absence include biophysical (TNA, temperature annual range, dry quarter precipitation), anthropogenic (minimum distance to towns and roads) and composite (NDVI) variables. The extensive and ongoing land cover transformation of this region, from forest to pasture and agriculture, will likely increase the extent of burned areas and future carbon fire emissions to the atmosphere.

© 2017 Elsevier Ltd. All rights reserved.

1. Introduction

Fire is an important disturbance agent for terrestrial ecosystems, particularly in tropical and subtropical regions (Giglio et al., 2010). Fire occurrence is controlled by multiple biophysical and anthropogenic variables (e.g. Chuvieco, Giglio, & Justice, 2008a; Bowman et al., 2009; Oliveira, Pereira, San-Miguel-Ayanz, & Lourenço, 2014). For instance, several studies show that fires exhibit large intra and interannual variability, and that these patterns are related to annual rainfall, seasonality and longer-scale climate oscillations such as ENSO (Bowman et al., 2009; Kitzberger, Swetnam, & Veblen, 2001; van der Werf et al., 2008, 2006). Other biophysical variables affecting fire occurrence include fuel type, vegetation structure, and topography (Bowman et al., 2009). In developing countries, fire is

commonly used for forest clearing, and as a land management practice for agriculture and cattle ranching (Cochrane et al., 1999, van der Werf et al., 2008; Armenteras & Retana, 2012; Lima et al., 2012). Fire is also considered an important factor affecting climate change through its effects on the cycle of several trace gases in the atmosphere, including CO₂ and CH₄ (Langenfelds et al., 2002; van der Werf, Randerson, Collatz, & Giglio, 2003). Climate change, in turn, may lead to more frequent and intense fire occurrences, because of increased temperatures and more extreme droughts (Giglio et al., 2010).

Global analyses of fire patterns show that the tropics are critical as they exhibit the highest densities of fire occurrence and contribute significantly to global fire carbon emissions (van der Werf et al., 2008, 2010, 2006; Chuvieco et al., 2008a; Langenfelds et al., 2002). For instance, total carbon emissions from fires in SE Asia for the 1997–1998 El Niño event were estimated to represent ~40% of global fossil fuel emissions for that period (van der Werf et al., 2008). For Latin America, a regional analysis revealed that

* Corresponding author. Departamento de Historia y Ciencias Sociales, km 5 Via Puerto Colombia, Universidad del Norte, Barranquilla, Colombia.

E-mail address: nbotero@uninorte.edu.co (N. Hoyos).

153,215 km² of land were burned from December 2003 to December 2004. Countries most affected included Cuba, Colombia, Venezuela, Bolivia and Argentina (Chuvienco et al., 2008b). A large percentage of burned scars (63%) were located in grasslands and savannas (Chuvienco et al., 2008b). National and regional analyses for Colombia indicate that fires exhibit a strong spatial and temporal pattern related to multiple biophysical and anthropogenic variables (Armenteras & Retana, 2012; Armenteras et al., 2011, 2005; Borrelli, Armenteras, Panagos, Modugno, & Shütt, 2015; Romero-Ruiz, Etter, Sarmiento, & Tansey, 2010). Regions most affected by fires include the country's eastern llanos, the eastern Andean footslopes and the Caribbean region (Armenteras et al., 2011). Explanatory variables differ from one region to another, underscoring the importance of conducting analysis at the regional scale (Chuvienco et al., 2008b).

Colombia experienced in 2015 the strongest El Niño conditions since 1997–1998, according to the National Institute of Hydrology, Meteorology and Environment (IDEAM, in Semana, 2016). Dry conditions associated with this event favored the occurrence of a large number of fires (National Office for Risk Disaster Management, in Semana, 2016) which affected ~120,000 ha of land at the national level, including ~23,000 ha of forests (Calderón, Romero, & Alterio, 2015, p. 5). Loss of forest ecosystem services due to fires, including wood and hydrologic regulation, was estimated at ~US\$176 million for the entire country (0.063% of 2015 GDP; Calderón et al., 2015, p. 5). In terms of water deficits, the Caribbean region experienced the largest rainfall deficit during 2015, ranging between 48 and 78% (IDEAM, in El Tiempo 2015). This region is particularly vulnerable to fire occurrence due to large seasonal

water deficits, even during average climatic conditions, as well as high interannual rainfall variability (Restrepo et al., 2014). Previous studies on fire activity in Colombia have identified the eastern llanos as the region where fires occur most frequently, followed by the Amazon and the Caribbean regions (Armenteras, González-Alonso, & Franco, 2009, 2011, 2005; Romero-Ruiz et al., 2010). A detailed regional analysis of the Caribbean region is required because the area (1) possesses endangered ecosystems such as tropical dry forests, and (2) displays unique interactions between biophysical and anthropic factors, e.g. land-use practices (Armenteras et al., 2011). Ultimately, the Caribbean region of Colombia will prove to be critical for the future sustainability of tropical dry forests, as it holds the largest and best preserved expanses of this ecosystem type nationwide (García, Corzo, Isaacs, & Etter, 2014).

We analyzed fire patterns of the Colombian Caribbean between 2003 and 2015, aiming to determine the environmental envelope (i.e. biophysical and anthropogenic conditions) under which the occurrence of fire is most likely. Accordingly, we addressed two research questions: (1) what are the seasonal and interannual patterns of fires in the region? and (2) which biophysical and anthropogenic variables better explain the occurrence of fires?

2. Study area

The Caribbean region of Colombia covers an area of approximately 139,300 km², stretching between the borders with Panama to the west and Venezuela to the east (Fig. 1). Most of the region sits on low relief Tertiary sedimentary sequences and Quaternary

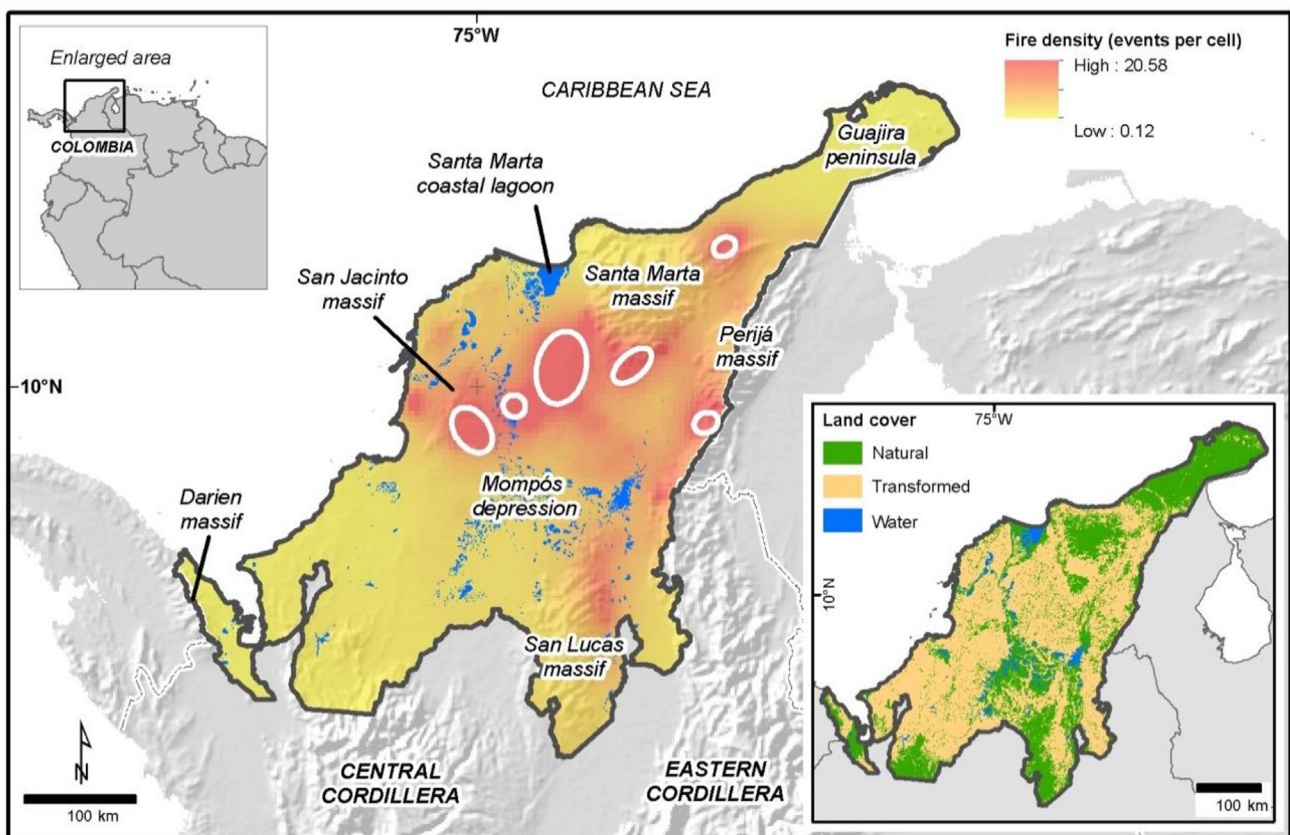


Fig. 1. Location of our study area, showing relevant geographic features and areas with high density of fire detections for the 2003–2015 period (cell area of 25 km²). Significant hotspot areas are shown as 1.5 standard deviational ellipses (white outline). Inset shows extent of land cover transformation (MADS et al., 2015). Elevation data from ETOPO1 dataset (Amante & Eakins, 2009).

alluvial deposits (Servicio Geológico Colombiano, 2015). The northern Guajira peninsula has several small isolated massifs of Proterozoic, Paleozoic and Mesozoic crystalline rocks (Weber et al., 2010). Further south is the Santa Marta massif (SNSM hereafter), a 5770 m triangular high made of metamorphic and intrusive rocks of Proterozoic through Paleogene age (Tschanz, Marvin, Cruz, Mehnert, & Cebula, 1974; Cardona et al., 2011). East of the Santa Marta massif is the N-S elongated Perijá massif, made of Jurassic volcanic and volcanoclastic rocks overlain by a Cretaceous carbonate sequence (Montes et al., 2010). Running parallel to the coast, with a N-NE direction, are the Sinú and San Jacinto volcano-sedimentary deformed belts of Cretaceous and Cenozoic age (Guzmán, Gómez, & Serrano, 2004), which form low relief massifs such as the San Jacinto massif. On the southern edge of our study area is the San Lucas massif, a northern extension of the central Andean cordillera. Finally, along the Panama border sits the Darien massif made of Cretaceous and Tertiary igneous rocks (Servicio Geológico Colombiano, 2015).

Climate is modulated at the annual scale by the movement of the Intertropical Convergence Zone (ITCZ) (Poveda, Waylen, & Pulwarty, 2006). The southward movement of the ITCZ brings dry conditions to the Colombian Caribbean during the months of December through March (Poveda et al., 2006), with monthly precipitation below 50 mm throughout most of the region (January–February) and strong easterly trade winds (IDEAM., 2015). During the northern hemisphere's summer, the ITCZ shifts northwards and the Colombian Caribbean region experiences a wet season (September–November) with weak winds of variable direction and intense cyclonic activity (IDEAM., 2015). Precipitation for the wettest month (November) ranges from 50 mm (Guajira peninsula) to 400 mm near the Panama border (IDEAM., 2015). Other sources of rainfall variability are westerly (Chocó) and northerly (San Andrés) jet streams (Bernal, Poveda, Roldán, & Andrade, 2006; Poveda & Mesa, 2000). The former produces moisture advection from the Pacific Ocean into western Colombia, promoting intense rainfall due to orographic uplift on the slopes of the Western Cordillera (Poveda & Mesa, 2000). Its seasonal strengthening coincides with the main rainy season of October–November (Poveda et al., 2006). On the other hand, the San Andrés Jet is associated with the easterly trade winds, with a seasonal strengthening during the dry seasons of December–February and June–August (Bernal et al., 2006). As a result, annual rainfall in the region exhibits large spatial variation, with values as low as 300 mm in the northeastern Guajira peninsula, to ~2000 mm in the southwestern Darien region near the Panama border (IDEAM., 2015). Interannual rainfall variability is related to several ocean-atmosphere oscillations, including El Niño/Southern Oscillation (ENSO), the Quasi-biennial oscillation (QBO), and the Tropical North Atlantic index (TNA). In Colombia, the occurrence of El Niño (warm phase of ENSO) is associated with dry conditions, particularly in the Pacific and Andean regions, while La Niña (cool phase) has the opposite effect (Poveda, Jaramillo, Gil, Quiceno, & Mantilla, 2001). The QBO involves oscillations in the direction of zonal winds and temperature, and shows a weak, non-linear effect on rainfall in the country, but can modulate the magnitude and intensity of ENSO events (Mesa, Poveda, & Carvajal, 1997; Poveda, 2004). The TNA reflects sea surface temperature anomalies in the tropical North Atlantic and affects rainfall and discharge in the Caribbean, particularly through interaction with ENSO events (Enfield & Alfaro, 1999; Restrepo et al., 2014). Mean annual temperature in the region fluctuates between 26° and 30 °C in the lowlands, with little variation throughout the year.

Terrestrial vegetation ranges from xerophytic in Guajira and other northern coastal areas, to lowland moist forest in Darien. Remnants of lowland dry forest are found mostly on the foothills of

the Santa Marta, Perijá and San Jacinto massifs (García et al., 2014). Subandean and Andean forests are found mostly in the Santa Marta massif, as well as tropical high altitude grasslands or páramos (MADS et al., 2015). Wetlands occur along the floodplains of major rivers and in the coastal fringe. In particular, there are extensive freshwater wetlands in the Mompox tectonic depression of the lower Magdalena river, and mangrove forests around the Santa Marta lagoon (Jaramillo, Cortés-Duque, & Flórez, 2015, Fig. 1). Most of the original vegetation, however, has been transformed. There is evidence of environmental transformation by indigenous groups at least since ~1000 BCE, including the use of raised fields for agriculture in the Mompox Depression and slash-and-burn agriculture in the hills (Parsons and Bowen, 1966; Plazas, Falchetti, Sáenz, & Archila, 1993; Zambrano, 2000, Fig. 1). During the Spanish conquest, natural forest regeneration took place as the indigenous population was decimated (Parsons and Bowen, 1966; Ocampo, 2007). During the colonial period (1500–1800), cattle introduced by Europeans grazed freely in the natural grasslands and in secondary regrowth of cleared vegetation (Etter, McAlpine, & Possingham, 2008). Widespread colonization of the region did not start until the second half of the 1700s. As a result, by 1850 there was still considerable forest cover (Ocampo, 2007). This period was followed by drastic land transformation that continued into the 1900s, with commercial deforestation and rapid expansion of pasture for cattle ranching (Etter et al., 2008; Ocampo, 2007; Parsons, 1952; Posada-Carbó, 1996; Van Ausdal, 2009, pp. 126–149). National estimates show that by the year 2000, ~41 Mha of land (40% of the country) had been transformed, and that cattle grazing dominated about 75% of the transformed landscapes (Etter et al., 2008). At the regional level, the National Ecosystems Map shows that 60% of the original vegetation in the Caribbean has been transformed, and that half of the converted area has gone to pasture for cattle ranching (MADS et al., 2015; Fig. 1).

3. Methods

3.1. Datasets

A dataset containing fire occurrence data and associated biophysical and anthropogenic variables was generated for the 2003–2015 period. Variables included climate, vegetation, topography and human influence, as described below. Further details are included in Table 1.

- (1) *Active fire detections*. A fire dataset covering the period from January 2003 through December 2015 was obtained from MODIS active fire detections standard product (MCD14ML), distributed by NASA FIRMS (<http://firms.modaps.eosdis.nasa.gov/download/>). In this dataset, each point represents the center of a 1 km pixel flagged as containing one or more active fires at the time of the satellite overpass (Giglio, Descloitres, Justice, & Kaufman, 2003, <https://earthdata.nasa.gov/firms-faq#ed-modis-fire-onground>). Limitations of this product include no fire detection due to cloud cover, heavy smoke and dense tree canopy, fire occurrence in between satellite overpasses, or fires too small or too cool (Giglio, 2013). Each fire detection has a confidence value ranging from 0% (lowest confidence) to 100% (highest confidence; Giglio, 2013). We selected fire detections with confidence values $\geq 80\%$ (high confidence class) in order to minimize the number of false alarms (Giglio, 2013). We also discarded fire detections from coal mines, built-up areas (urban and industrial) and bare surfaces (e.g. sand bars).
- (2) *NDVI (normalized difference vegetation index)* was derived from MODIS MOD13Q product, retrieved from the online

Table 1
Dataset characteristics and derived variables used in our analysis.

Dataset	Spatial resolution	Temporal resolution	Sensor/Dataset	Source	Variables used
Fire	Point at the center of a 1 km pixel	1–2 days	Terra and Aqua MODIS/Collection 5.1 MCD14ML fire product	NASA ^a	Fire date and X/Y coordinates
NDVI	250 m	16 day compositing period	Terra MODIS/MOD13Q1 V005	NASA ^b	NDVI
Elevation	250 m	N/A	GMTED2010	USGS ^c	Elevation Slope Aspect
Towns	N/A	N/A	N/A	IGAC, IBVSB, Panama Environmental Ministry ^d	Distance to town Distance to state capital
Rivers, lakes, roads	N/A	N/A	N/A	IGAC ^d , Digital chart of the world ^e , MADS et al., 2015	Distance to water Distance to road
Unsatisfied basic needs index	N/A	Municipal, urban, rural and overall, year 2010.	N/A	DANE ^f	Urban index Rural index Overall index
Bioclimatic variables	1 × 1 km	Representative of 1950–2000	N/A	Hijmans et al., 2005	bio1 = Annual Mean Temperature bio2 = Mean Diurnal Range bio3 = Isothermality (bio2/bio7) (* 100) bio4 = Temperature Seasonality (standard deviation *100) bio5 = Max. Temperature of Warmest Month bio6 = Min. Temperature of Coldest Month bio7 = Temperature Annual Range (bio5- bio6) bio8 = Mean Temperature of Wettest Quarter bio9 = Mean Temperature of Driest Quarter bio10 = Mean Temperature of Warmest Quarter bio11 = Mean Temperature of Coldest Quarter bio12 = Annual Precipitation bio13 = Precipitation of Wettest Month bio14 = Precipitation of Driest Month bio15 = Precipitation Seasonality (Coefficient of Variation) bio16 = Precipitation of Wettest Quarter bio17 = Precipitation of Driest Quarter bio18 = Precipitation of Warmest Quarter bio19 = Precipitation of Coldest Quarter
Climate indices	N/A	Monthly, bimonthly	N/A	NOAA ^g	TNA QBO MEI
Ecosystems/land cover	1:100.000	2015	N/A	MADS et al., 2015	

^a <https://firms.modaps.eosdis.nasa.gov/download/>.

^b <http://reverb.echo.nasa.gov/reverb/>.

^c <http://earthexplorer.usgs.gov/>.

^d IGAC (Colombia's Geographic Institute), IBVSB (Venezuela's Geographic Institute), Panama Environmental Ministry.

^e https://worldmap.harvard.edu/data/geonode:Digital_Chart_of_the_World.

^f Colombia's National Statistics Department, downloadable from the national GIS portal at <http://sigotn.igac.gov.co/sigot/>.

^g <http://www.esrl.noaa.gov/psd/data/climateindices/list/>.

Reverb ECHO tool from NASA. We downloaded 16-day composite images from January 2003 through December 2015 with a spatial resolution of 250 m. The entire region was covered by 3 images which we subsequently mosaicked for each period, resulting in 299 mosaics. This variable was intended to represent vegetation conditions within 15 days of each fire's occurrence. Although there are several parameters to evaluate the quality of NDVI data, we paid special attention to the usefulness parameter, which is ranked from 0 (highest quality) to 12 (not useful). From all fire detections analyzed, 83.61% had a high NDVI usefulness score (0–4), 15.89% had an intermediate score (5–8), and only 0.5% had a low score (above 8). We decided to use all data points for the analyses, considering that low usefulness scores represented a very low proportion of the dataset, and in case statistical relationships resulted significant these would prove robust.

(3) *Elevation* data was obtained from the GMTED2010 dataset, available from the U.S. Geological Survey (<https://lta.cr.usgs.gov/GMTED2010>) at 7.5 arc-second spatial resolution. The study area was covered by 2 images which we mosaicked and projected to UTM coordinates with a pixel size of 250 m. We used elevation to generate slope and aspect rasters with the same spatial resolution.

(4) *Towns, roads and rivers datasets* were obtained from multiple sources for the Colombian Caribbean as well as neighboring regions in Panamá and Venezuela. These datasets were used to generate distance rasters with the same spatial resolution as NDVI mosaics. Towns were split into state capitals and towns, and separate distance rasters were derived for each of them. Distance to towns and roads was intended to represent the effect of population and infrastructure on fire occurrence. Distance to rivers was included because of its relation to multiple conditions such as soil moisture and land cover/land use.

(5) *Unsatisfied basic needs index* as calculated by the Colombian National Statistics Department (DANE). This index is

Table 2

Techniques and parameters used for point analysis. Further details for parameters are provided in Levine (2013).

Technique	Parameters
Spatial and temporal analysis of crime (STAC)	Search radius: 10 km Minimum number of points per cluster: 300. Output: Standard deviational ellipse (1.5 standard deviations)
Single kernel density	Kernel function: Normal Bandwidth: Adaptive (minimum number of points set to 100) Density calculation: Absolute (events per grid cell)

calculated for urban and rural areas within each municipality, as well as an average for the municipality as a whole. It represents the percentage of the municipal population (total, urban or rural, respectively) lacking one or more of the following basic needs: adequate and uncrowded housing conditions, utilities (water supply, sewage, garbage disposal), economic means, and children school attendance. Our assumption was that fire occurrence would differ between areas with high values for this index (few economic resources, usually remote) and those with low values.

- (6) *Bioclimatic (bioclim) variables* were obtained from <http://www.worldclim.org/> (Hijmans, Cameron, Parra, Jones, & Jarvis, 2005). These variables are calculated from observed temperature and precipitation data for the period 1950–2000. They represent annual and seasonal trends as well as extreme conditions
- (7) *Climate indices* were obtained from NOAA (<http://www.esrl.noaa.gov/psd/data/climateindices/list/>). We used the following indices as they are related to rainfall variability in the region at different time-scales (Enfield & Alfaro, 1999; Mélice & Servain, 2003; Restrepo et al., 2014): MEI (multivariate ENSO index), TNA (Tropical North Atlantic index) and QBO (Quasi-biennial oscillation)

3.2. Data analyses

We used the following approaches for data analysis: (1) temporal approach for variables that changed over time (i.e. fire detections, climate indices and NDVI), and (2) spatial approach for variables that had a spatial component (all except climate indices).

Temporal patterns of fire events. We analyzed fire frequency at the monthly, seasonal and annual time scales. We defined the dry seasons from December through March and from June through August, and the wet seasons from April through May and from September through November (Restrepo et al., 2014). Although there are local variations to this seasonal pattern, we consider it representative of most of our study region. Analyses were conducted with NCSS 9 statistical software (Hintze, 2013). We performed time series decomposition for fire detections and climate indices to express the observed data series in terms of their long-term trend, seasonal, and random components. We also used cross correlation analysis between fire detections and other temporal variables (climate indices and NDVI) to evaluate the timing and nature of their association. Fire detections and QBO were log-transformed to meet the normality assumption. These analyses were performed in R (R Core Team 2016).

Spatial patterns of fire events and the environmental envelope of fire occurrence. We used hotspot detection and density analysis techniques to test whether fires had a random or clustered spatial distribution. Hotspot techniques identify clusters or concentrations for the data points themselves, while density techniques generalize those points to the entire study region. Specifically, we used a hotspot detection technique that combines a scan-type algorithm

in which the number of events within a moving circle is counted, with hierarchical clustering where points in overlapping clusters are combined into a larger cluster (STAC; Levine, 2013). Its output is a standard deviational ellipse computed for the points identified to be a “hot spot”. On the other hand, we used single kernel density to generate a surface of fire density for our study region. For each technique, we systematically tested different parameters until we obtained a regional pattern (rather than a local one; Table 2). Analyses were performed in CrimeStat v 4.02 (Levine, 2015), a free application originally developed for crime analysis that offers multiple spatial statistical techniques for the analysis of point distributions, and generates outputs to different geographic information systems. We used ArcGIS (ESRI, 2014) for the visualization of results.

Once we determined that fires were not randomly distributed, we generated a no-fire dataset to estimate the probability of fire occurrence given the observed environmental gradients (Fig. 2). The no-fire dataset was composed of a random set of points ($n = 19,800$) that was generated by excluding areas where fires were detected. For this purpose, we first selected years with contrasting fire detections and climatic conditions: high number of fire events and dry conditions (years 2003, 2015), low number of fire events and wet conditions (years 2010, 2011), median fire events and average rainfall (year 2009). For every month within these five years, we generated a no-fire polygon by placing a 5 km radius buffer around each fire occurrence (i.e. fire areas), including all detections regardless of their confidence level ($n = 66,975$). These areas, as well as bare and built-up areas, coal mines and water bodies were masked out from the study region polygon to obtain a monthly no-fire polygon. Each of these monthly no-fire polygons was randomly sampled for 330 points, totaling 19,800 no-fire points, a sample size intended to balance the number of fire points analyzed. Each no-fire point was arbitrarily assigned to the 15th day of its respective month for subsequent data extraction. Under this procedure, no-fire points might be the result of cloud cover, however, we consider that this should not be a major issue for most of the study area because (1) most fires take place in the dry season (January to March) when cloud cover is minimal, and (2) the average number of days without sunshine, an indirect measurement of cloud cover available from the National Climate Atlas (IDEAM, 2015; not shown), indicates that our study region is not characterized by persistent cloud cover, even during the wet seasons. In any case, if spurious non-fire point detection were a substantial component of the dataset, its effect would probably reflect in non-significant statistical relationships with environmental variables.

For all points in the fire and no-fire datasets, we extracted values for NDVI, topographic, and distance variables by placing a 1×1 km window around each point and calculating the mean, maximum and minimum value within the window (Fig. 2). We used this sampling strategy because each fire occurrence represented the center of a 1×1 km cell, while raster data had a 250 m spatial resolution. NDVI values accounted for each point's date of occurrence since each NDVI image spanned a 16-day period. Bioclimatic

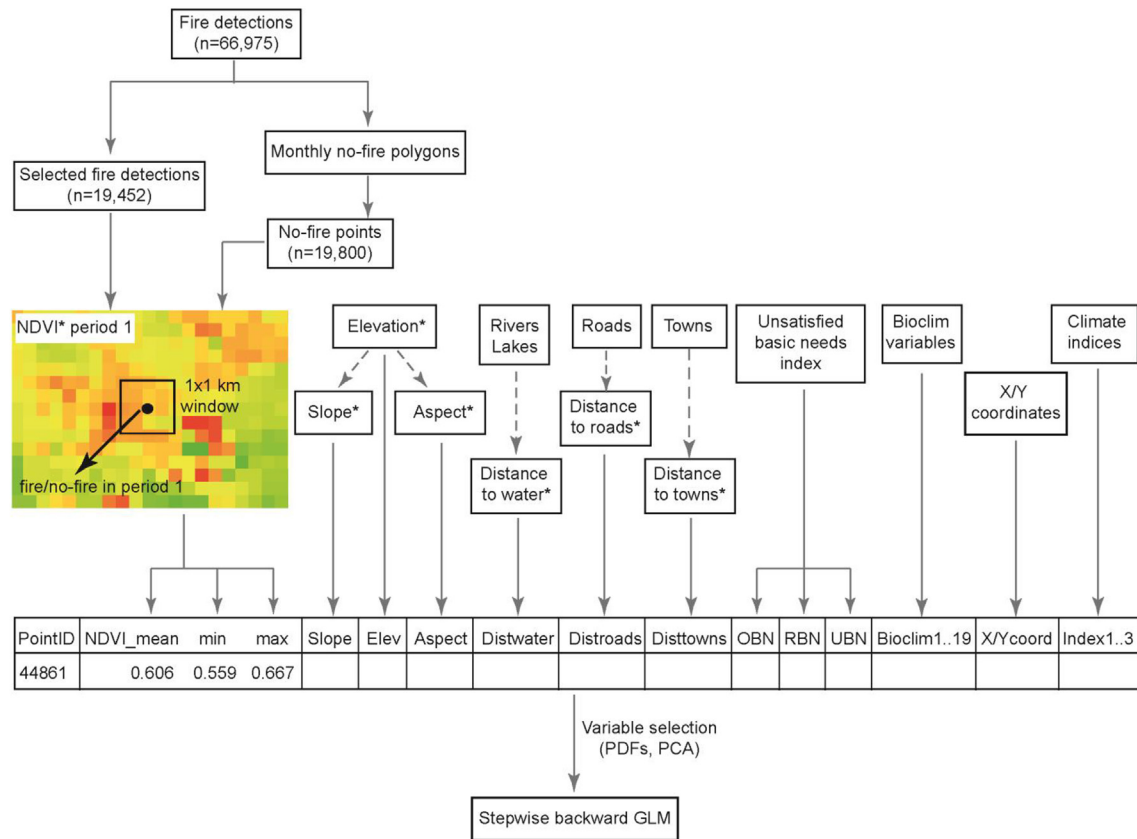


Fig. 2. Summary of methods used to generate the GLM input dataset. Variable extraction was performed for each of the fire and no-fire points. The 1 × 1 km window is shown for NDVI but was used for all variables marked with an asterisk (*). Dashed arrows point to variables derived from the datasets listed in Table 1 (OBN = overall unsatisfied basic needs index, RBN = rural unsatisfied basic needs index, UBN: urban unsatisfied basic needs index, Bioclim = bioclimatic variables). Notation for bioclim and climate indices represents the number of variables associated with each (e.g. 19 bioclimatic variables and 3 climatic indices). PDFs = probability density functions, PCA = principal component analysis.

variable values were assigned directly to each point, as these variables had a spatial resolution of 1 × 1 km. Values for unsatisfied basic needs index were assigned to each point based on its municipality, while climate indices were assigned based on each point's date of occurrence. Finally, we also extracted the X and Y coordinates for all points. These were included in the analysis for two main reasons: (1) climatic and anthropogenic variables tend to follow a systematic pattern in space, and therefore these variables could eventually serve as surrogates for many other variables, and (2) these variables are expected to be highly useful for the purpose of predicting. All data extraction was performed with a customized Python script (Python Software Foundation, 2016) within ArcGIS arcpy package (ESRI, 2014).

A logistic generalized linear model (GLM) was used to quantify the effect of biophysical and anthropogenic variables on fire occurrence probability. For estimating the model, we selected a group of independent variables based on two criteria: (1) a clear differentiation of the probability density function (PDF) of each variable under fire and no-fire points, and (2) non-redundancy as determined by a principal component analysis (PCA). PDFs are generalizations of the empirical distribution of data (Venables & Ripley, 2002). In our case, PDFs represent the frequency of environmental variables under the fire and no-fire scenarios. PCA is a multivariate technique that can be used as redundancy analysis tool to identify the relative contribution of variables to the total variance of the dataset, and the relationships among variables (Legendre & Legendre, 1998). All selected variables were used to fit the logistic model, and then a stepwise backward variable selection was used to trim the model. We chose the best model based on its

explanatory and predictive power (percentage of false positives and false negatives), and the Akaike information criterion (AIC; Akaike, 1974). All analyses were performed in R (R Core Team 2016).

4. Results

4.1. Temporal patterns of fire events

Over the entire study period there were 19,452 active fire occurrences with a confidence level above 80. The analysis of monthly fire frequency revealed that the vast majority of fire detections occur between February and March (~82%), with March having 60% of all detections. This pattern was reflected at the seasonal scale, with 86% of fire detections taking place during the main dry season of December through March. Accordingly, our time series analysis shows a distinctive seasonal cycle, with a clear positive peak that matches the main dry season of December–March (Fig. 3a). Fires also show large interannual variability, with 2003 having the highest number of fire detections (~16%) while 2011 having the lowest (~1%) (Fig. 3a). TNA also showed a clear annual signal with a distinctive peak towards the end of the year. In addition, TNA had a downward trend between 2005 and 2009, followed by a sharp peak in 2010–2011 (Fig. 3b).

Cross correlation analysis for fire detections and NDVI revealed both, significant positive and negative correlations over diverse lags. Low NDVI values were associated with high fire detections at lags of 0, 5, 10, 11, and 12 months, implying that under these time frames, low vegetation vigor was associated with high fire frequency. Significant positive correlation between NDVI and fire

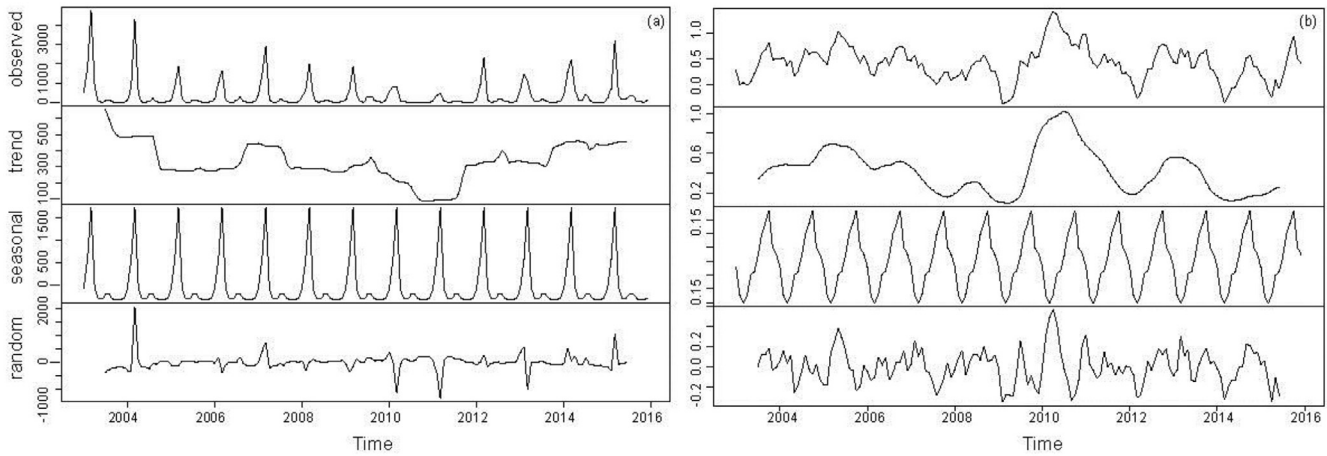


Fig. 3. Decomposition of additive time series for (a) active fires, and (b) Tropical North Atlantic Oscillation Index (TNA). For both datasets, the upper panel represents the observed time series, whereas the lower panels represent their additive components (long-term trend, seasonal, and random components, respectively, which together add up to the observed data) in the same units than the original dataset (number of fire detections for the left side panels, and TNA index in the right side panels).

detections were detected at lags of 7 and 8 months, meaning that high NDVI values were correlated with high fire detections 7–8 months later (Fig. 4a). Overall, considering backward lags, the association between NDVI and fire occurrence was significant at a quarterly scale, switching sign between consecutive quarters. Fire detections and TNA showed significant correlation at lags between 0 and 3, and between 10 and 12 months, i.e. low TNA values were associated with high fire occurrences (Fig. 4b). Overall, considering backward lags, TNA and fire were significantly associated every six months, switching sign every semester. Cross correlations for active fires, MEI and QBO were not significant.

4.2. Spatial patterns of fire events and fire environmental envelope

Hotspot and density analyses revealed several regions with a high concentration of fire occurrences, namely the southern and northern foothills of the Santa Marta massif, plains to the southwest of the Santa Marta massif, eastern foothills of the San Jacinto massif, and the Perijá massif near the Venezuelan border (Fig. 1).

We selected a preliminary group of 20 variables (out of 48) based on visual comparison of PDFs for fire and no-fire points, and expert knowledge. Probability density functions revealed differences between fire and no-fire points for most of these variables.

For instance, NDVI exhibited higher fire probability at mean values of ~0.4, while higher no-fire probability at mean values of ~0.8, i.e. fires were more likely to occur at lower NDVI values (Fig. 5). PDFs for climate related variables such as mean temperature annual range (bio7), precipitation seasonality (bio15), precipitation of the driest quarter (bio17) and TNA also revealed differences between fire and no-fire points. For instance, fires had a higher probability, compared to no-fires, at lower TNA and precipitation seasonality values. Fires were also more likely to occur when precipitation of the driest quarter was ~100 mm, while they were less likely to occur when this variable reached values above 200 mm. Location variables showed that no-fires were more likely to occur, compared to fires, at the southern and northern boundaries of our study area. Along the west-east direction, both fires and no-fires were more likely to occur at the center of our study area. On the other hand, there were some variables that showed little difference between fire and no-fire points, such as distance to roads and unsatisfied basic needs index.

Principal component analysis performed on the preliminary selection of 20 variables showed redundancy among some bioclimatic variables, and climate indices (Fig. 5). Based on the characteristics of our study area, we selected variables that: (1) represented precipitation seasonality (bio 15, bio17, TNA), (2) were

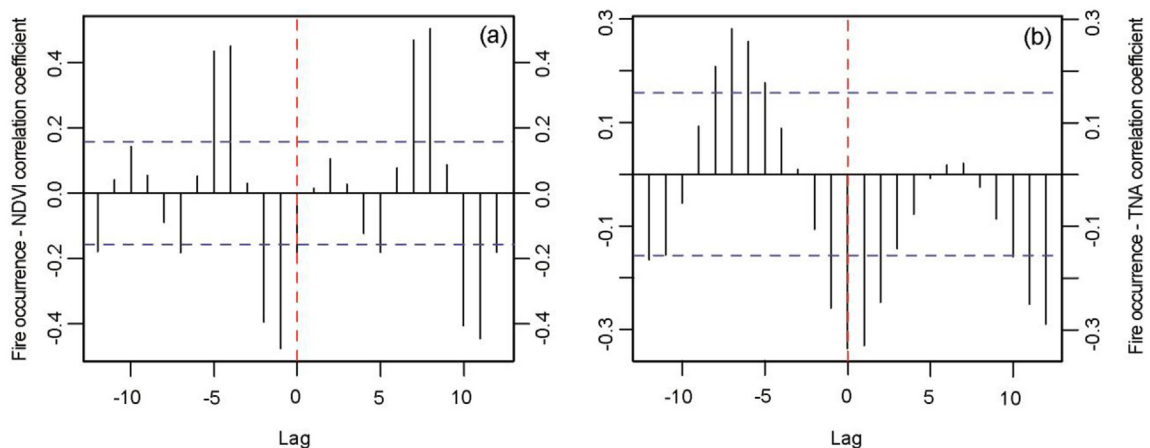


Fig. 4. Cross correlation function for (a) fire detections and NDVI, (b) fire detections and Tropical North Atlantic Oscillation Index (TNA). Horizontal dashed line represents the 95% significance level (n = 19,452), lag in months.

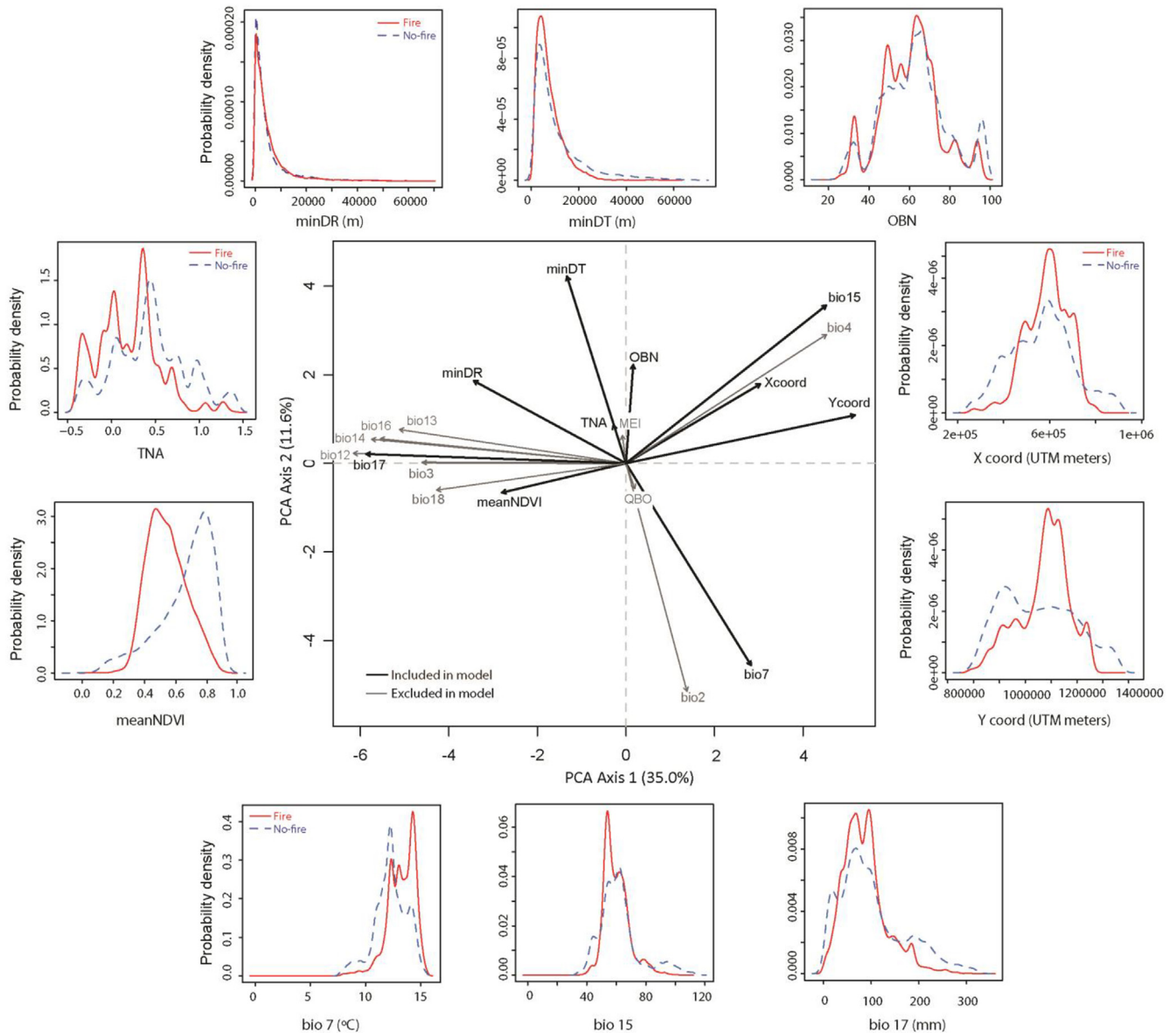


Fig. 5. Principal component analysis (PCA) plot and probability density functions (PDFs) for selected independent variables. PCA plot includes variables preliminarily selected based on their PDFs and expert knowledge. PDFs are only shown for the 10 variables used as input for the GLM. minDR = minimum distance to road, minDT = minimum distance to town, OBN = overall municipal unsatisfied basic needs index, bio7 = temperature annual range, bio15 = precipitation seasonality, bio17 = precipitation of driest quarter, TNA = North Atlantic Oscillation Index. Codes for other bioclimatic variables in Table 1.

uncorrelated, based on the PCA plot (bio 7, distance variables, unsatisfied basic needs index, X and Y coordinates), and (3) had the best temporal and spatial resolution (NDVI). As a result, we obtained a group of 10 independent variables that we used as input for the GLM model. A model with eight independent variables was selected, because it had high explanatory power (~76.4%), the lowest percentage of false positives (~11.8%), and one of the lowest AIC (Table 3, Fig. 6). This model was:

$$\begin{aligned}
 \text{Fire Probability} = \text{logit}^{-1} & (\beta_0 + \beta_1 \text{meanNDVI} + \beta_2 \text{bio7} + \beta_3 \text{TNA} \\
 & + \beta_4 \text{minDT} + \beta_5 \text{minDR} + \beta_6 \text{bio17} \\
 & + \beta_7 \text{Xcoord} + \beta_8 \text{bio15})
 \end{aligned}$$

Independent variables with an inverse relationship with fire probability included NDVI, TNA, minimum distance to towns,

precipitation of driest quarter and precipitation seasonality. By comparison, temperature annual range, minimum distance to roads and X coordinate had a positive relationship with fire probability (Fig. 7). Given that geographic coordinates are specific to the study region, they cannot be treated as having the same effect on fire regimes at a global scale. They are just variables with the statistical potential to express the spatial configuration of other natural variables (e.g. precipitation, temperature, topography, etc.). In any case, given that the model was estimated for a specific range of dates, its use as predictor for other regions would not hold, as it would be an extrapolation.

5. Discussion

Our results confirm findings from other global and regional studies showing fire as a complex process affected by multiple

Table 3
Logistic generalized linear models to explain fire as a function of independent variables. In all cases, $\text{Logit}(\text{fire}) = X\beta$, where X corresponds to the explanatory variables selected for each model (bio7 = temperature annual range, minDT = minimum distance to town, minDR = minimum distance to road, bio17 = precipitation of driest quarter, bio15 = precipitation seasonality, OBN = overall unsatisfied basic needs index), and β are the estimated coefficients associated with each model. Each cell shows the estimated coefficient (upper line), and its standard error (lower line). The selected model is highlighted in grey.

Number of explanatory variables	β_0	meanNDVI	bio7	TNA	minDT	minDR	bio17	X coord	bio15	Y coord	OBN	AIC
10	1.757 0.290	-5.774 0.089	0.380 0.014	-1.522 0.033	-0.00007 0.000002	0.00006 0.000002	-0.005 0.000	0.000003 0.0000002	-0.047 0.003	-0.0000007 0.0000002	0.00044 0.00089	39317
9	1.638 0.283	-5.543 0.085	0.380 0.014	-1.524 0.033	-0.00007 0.000002	0.000065 0.000002	-0.005 0.0005	0.000003 0.0000002	-0.047 0.003	-0.0000008 0.0000002		39373
8	1.330 0.274	-5.503 0.085	0.360 0.013	-1.525 0.033	-0.00008 0.000002	0.00006 0.000002	-0.004 0.0005	0.000003 0.0000002	-0.050 0.003			39391
7	-3.237 0.141	-5.502 0.084	0.529 0.011	-1.529 0.033	-0.00008 0.000002	0.000067 0.000002	0.003 0.0003	0.0000006 0.0000001				39756
6	-3.097 0.138	-5.517 0.084	0.547 0.010	-1.526 0.033	-0.00008 0.000002	0.000068 0.000002	0.003 0.0003					39763
5	-2.898 0.137	-5.362 0.082	0.538 0.010	-1.536 0.033	-0.00008 0.000002	0.000077 0.000002						39880
4	-2.241 0.133	-4.667 0.077	0.465 0.009	-1.542 0.033	-0.00005 0.000002							41278
3	-3.816 0.125	-4.229 0.074	0.533 0.009	-1.558 0.032								42298
2	-3.883 0.122	-4.667 0.072	0.521 0.009									44904
1	2.907 0.044	-4.845 0.070										48774
0	-0.018 0.010											54415

biophysical and anthropogenic variables that work at different spatial and temporal scales (e.g. Hoffman, Schroeder, & Jackson, 2003, van der Werf et al., 2006, Chuvieco et al., 2008a; Bowman et al., 2009; Oliveira et al., 2014). From a global perspective, our study region is located within the highest fire density belt, corresponding to the tropics and subtropics between 20°N and 30°S with cyclical seasonal and interannual dry conditions (Chuvieco et al., 2008a). Regionally, Colombia is one of the countries most affected by fire in Latin America, with more than 1.2% (19,442 km²) of its territory burned between December 2003 and December 2004 (Chuvieco et al., 2008b). This value is most likely an underestimate, as ca. 30,000 km² of burned area were reported for the eastern Colombian llanos alone, between December 2003 and April 2004 (Romero-Ruiz et al., 2010).

5.1. Climate variables

Fires in the Colombian Caribbean are affected by regional and local climate processes related to intra-annual as well as interannual rainfall variability. Regional, low-periodicity climate oscillations (i.e. quasi-decadal TNA oscillation) show a significant correlation with fire activity in our study area. In comparison, more frequent oscillations such as ENSO and QBO were not significantly correlated with fire activity. The temporal structure of the correlations between fire occurrence and NDVI and TNA suggests that the association between fire and these variables manifests mostly through the regional seasonal cycle (Fig. 4). NDVI correlations were significant at a quasi-periodic quarterly time scale, whereas the association of TNA was quasi-periodic biannual. Whereas the former is probably associated with the flammability of the vegetation that depends on the bimodal distribution of precipitation (note the switch of the correlation sign between consecutive quarters), the latter corresponds to a more indirect effect of oceanographic cycles on precipitation seasonality. Indeed, results from our regression model indicate that fires are less likely to occur as TNA values increase (Fig. 7). Studies over Central America and Colombia show that both, TNA and ENSO, affect rainfall and

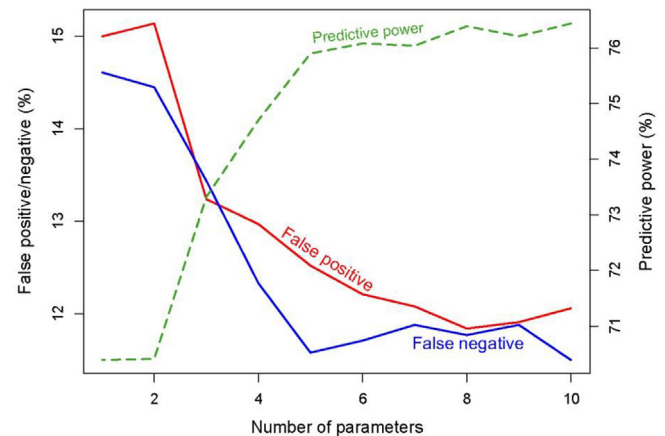


Fig. 6. Comparison of GLM performance. X axis shows model's number of independent variables. Selected model (model 8) has high predictive power and the lowest percentage of false positives.

discharge, but that ENSO's effect becomes weaker over the Caribbean and eastern regions of Colombia, as opposed to the Pacific and Andean regions (Enfield & Alfaro, 1999; Poveda et al., 2001; Restrepo et al., 2014). Specifically, large rainfall departures over the wider Caribbean and Central America occur when sea surface temperature (SST) anomalies over the tropical North Atlantic combine with oppositely signed SST anomalies in the tropical eastern Pacific (Enfield & Alfaro, 1999). These conditions took place in 2010, when large, positive TNA anomalies coincided with large, negative MEI anomalies (i.e. La Niña episode), leading to enhanced rainfall and stream flows (Restrepo et al., 2014), and low fire activity. On the other hand, years with high fire activity (2003, 2004, 2015) had both positive TNA and MEI anomalies. These results point to the complexity of the interactions between oscillatory signals of different periodicities, and their importance in explaining interannual rainfall variability in the region. On the other hand, intra-annual variability of fire activity in our study area is driven by the

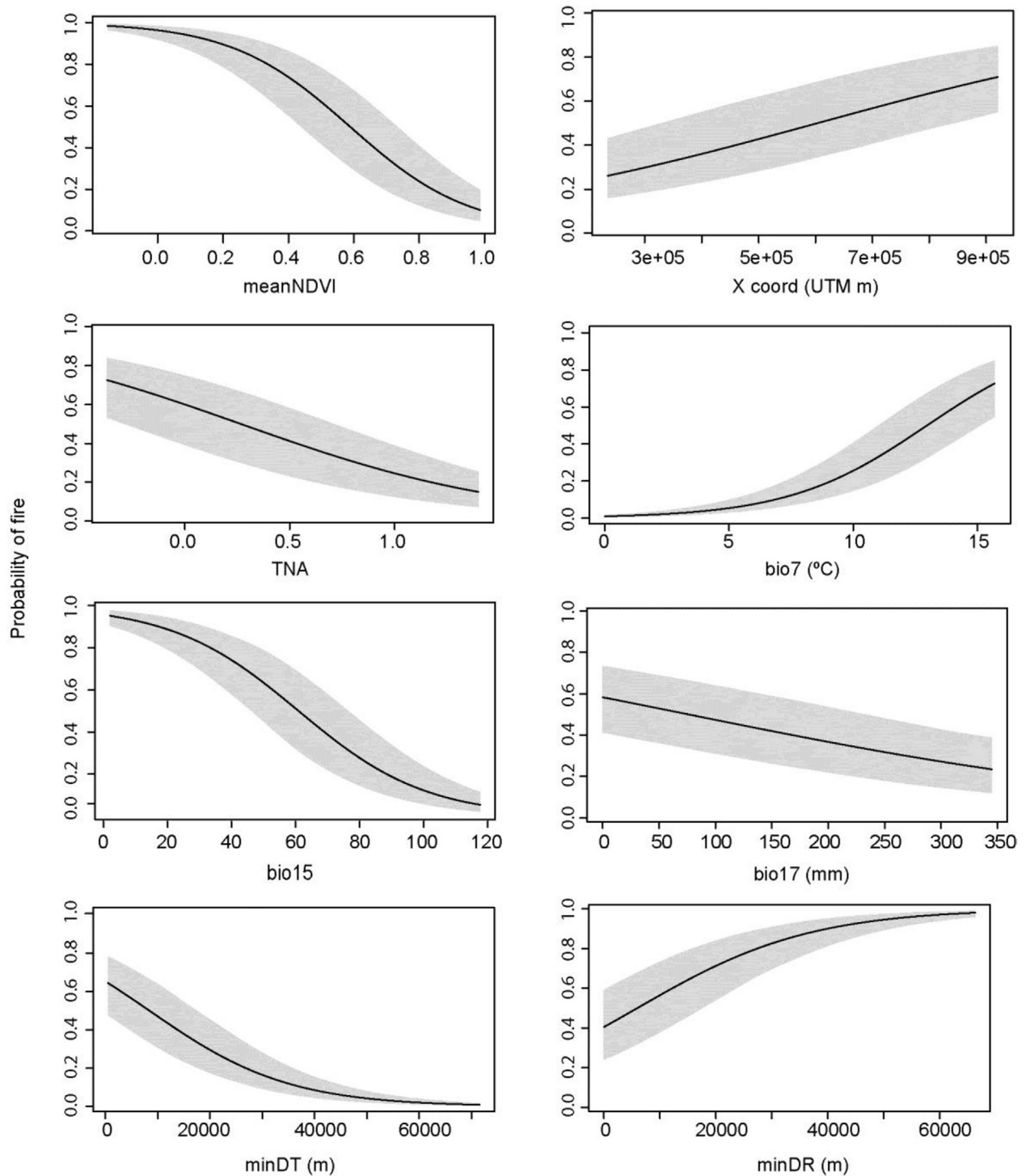


Fig. 7. Plots of selected model's independent variables (X axis) and fire probability (Y axis). Grey area represents 95% confidence level. TNA = North Atlantic Oscillation Index, bio7 = temperature annual range, bio15 = precipitation seasonality, bio17 = precipitation of driest quarter, minDT = minimum distance to town, minDR = minimum distance to road.

annual movement of the Intertropical Convergence Zone (ITCZ), as has been found in other tropical and subtropical regions (van der Werf et al., 2006; Chuvieco et al., 2008a; Armenteras et al., 2009, 2011; Romero-Ruiz et al., 2010). Accordingly, within any given year, most fires in the Colombian Caribbean occur during the main dry season of December–March.

Our regression model shows that regional temperature and

precipitation patterns affect fire probability, in particular temperature annual range (bio7), dry season precipitation (bio17) and precipitation seasonality (bio15). For instance, fires are more likely to occur where annual temperature range is high, with an average 9% increase in fire probability for every 1 °C increase in annual temperature range. Values for bio7 in our study area vary between 7.5 and ~16 °C, with the largest values occurring in the lowlands

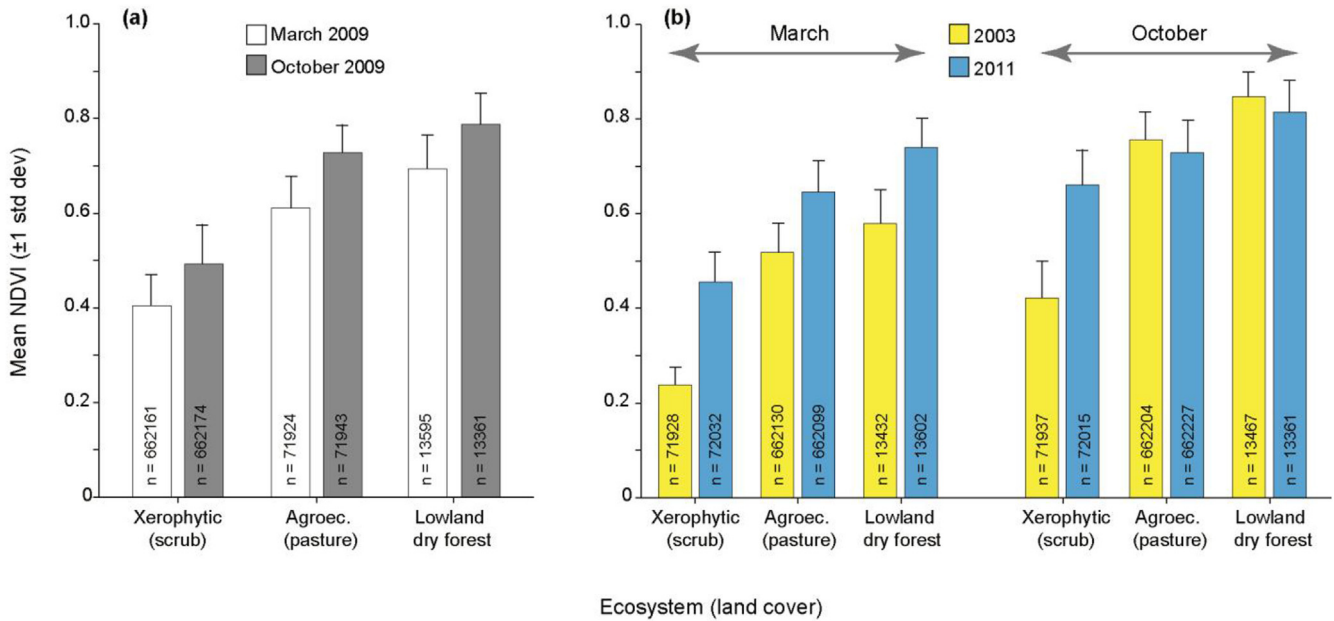


Fig. 8. Normalized difference vegetation index (NDVI) variability for three ecosystems within our study area: xerophytic, agroecosystems (pasture for cattle), and lowland dry forest. (a) Mean NDVI for March and October of 2009. This year had average precipitation and fire activity, (b) mean NDVI for March and October of 2003 (drier than average, highest fire count) and 2011 (wetter than average, lowest fire count). “n” refers to the number of sampled cells from the NDVI raster layer (250 m cell size). Error bars represent standard deviation. Ecosystems and land cover data from the National Ecosystems Map (MADS et al., 2015).

south of the SNSM, away from the coastline. This is the same area where most fire hotspots are located (Fig. 1). In terms of precipitation, fires are more likely to occur where dry quarter precipitation is low (Fig. 7). On average, fire probability increases by ~11% for every 100 mm decrease in dry quarter precipitation. The seasonally driest areas (<20 mm dry quarter precipitation) occur along the northern Caribbean coastline, excluding the SNSM, and the Guajira Peninsula. By comparison, the seasonally wettest areas (>350 mm dry quarter precipitation) are located on the SNSM and Andean foothills. Accordingly, fire density is higher in seasonally drier areas, except for the Guajira Peninsula, with the lowest dry quarter precipitation values. This region provides a good example of the multiple variables that affect fire occurrence. Annual precipitation in northern Guajira does not exceed 500 mm, and occurs mostly in September through November. Mean precipitation for the dry quarter (January through March) is 16 mm. As a result, the region has both, high precipitation seasonality and low dry quarter precipitation. This pattern is captured by the precipitation seasonality variable, showing decreasing fire probability with increasing precipitation seasonality (Fig. 7), contrary to results from other studies that show higher fire activity in seasonally dry areas (van der Werf et al., 2006; Chuvieco et al., 2008a, 2008b; Romero-Ruiz et al., 2010).

5.2. Anthropogenic and hybrid variables

Multiple anthropogenic variables have been related to fire activity, including deforestation in colonization fronts, distance to roads and towns, agricultural practices, livestock grazing, economic resources and land tenure (Hoffman et al., 2003; van der Werf et al., 2006; Chuvieco et al., 2008a; Bowman et al., 2009; Armenteras et al., 2011; Lima et al., 2012; Oliveira et al., 2014; Borrelli et al., 2015). Our model includes anthropogenic variables related to accessibility (distance to roads and towns), and one hybrid variable (NDVI) that summarizes climate, land cover and land use.

Distance variables included in our model show opposite effects, i.e. fire probability decreases away from towns, but it increases

away from roads (Fig. 7). On average, fire probability decreases by 1.9% for every 1 km increase in distance from a town. By comparison, fire probability increases on average 1.6% for every 1 km increase in distance from roads. A closer look at both layers reveals that most of our study area is close to towns and roads. Specifically, 63% of our study area is within 10 km of a town. Remote areas from towns include the northern Guajira peninsula, the highlands from the SNSM, Andean foothills, and part of Darien. On the other hand, 85% of our study area is within 10 km of a road, with remote areas being limited to the highlands of the SNSM, Perijá massif, Andean foothills and Darién. Other studies show that accessibility plays a significant role on fire occurrence, with areas near towns and roads showing higher fire frequency and lower interannual variability relative to remote areas (Borrelli et al., 2015; Chuvieco et al., 2008a; Kovacs, Ranson, Sun, & Kharuk, 2004). A closer look at the spatial distribution of distance values reveals that the northern Guajira Peninsula is driving the apparent inconsistency in our results. This region, with few fire occurrences, is far from towns, but not far from roads. In other words, our model is interpreting the patterns observed in northern Guajira as low fire probability being associated with proximity to roads but not with towns.

The relation between fire activity and NDVI reveals multiple temporal and spatial patterns. Based on our cross correlation analyses, NDVI effects on fire activity are complex, with both positive and negative correlations at different time lags. This pattern is related to the strong rainfall seasonality and resulting changes in NDVI within and between years. Fig. 8 shows mean NDVI values for three different land covers in our study area, i.e. scrub, pasture for cattle, and lowland dry forest. For 2009, a year with average precipitation and fire activity, NDVI values were consistently lower at the peak of the dry season (i.e. March), compared to the wet season (Fig. 8a). Interannual variability, on the other hand, can be assessed by comparing the months of March and October of 2003 and 2011 (Fig. 8b). Year 2003 was drier than average and had the highest fire count, while 2011 was wetter than average and had the lowest fire count. Mean NDVI for March was consistently lower for all land covers in 2003 compared to 2011, with scrub showing the largest

difference. The month of October, however, did not display the same pattern, as pasture and dry forest had slightly higher mean NDVI values in 2003 than in 2011.

According to our regression model, NDVI was the most significant variable in terms of its explanatory power (Table 3, Video). This is not surprising as this variable summarizes multiple climatic and anthropogenic effects. In addition, NDVI had the highest spatial and temporal resolution of all variables. In terms of fire probability, our model showed that, on average, fire probability decreases ~14% for every 0.1 unit increase in NDVI (Fig. 7). This relationship suggests that the extensive land cover/land use transformation of the Colombian Caribbean, from the former forested lowlands to pasture, would have led to an increase in burned area and fire carbon emissions. Studies show that clearing of humid tropical forests and savannas is associated with increased fire activity due to higher understory and surface temperatures and wind speeds, lower relative humidity and precipitation, and more rapid fuel drying (e.g. Cochrane et al., 1999; Hoffman et al., 2003). In addition to promoting temperature and humidity conditions favorable to fires, cattle ranching and agriculture also use periodic burning for pasture regeneration and crop planting. Other regional land use practices that promote fire are turtle hunting in wetlands, and coal production in mangrove forests (Vilardy, González, Martín-López, Oteros-Rozas, & Montes, 2012). Nevertheless, the effect of NDVI on the probability of fire occurrence, as modeled through the logistic GLM, has to be interpreted with caution, as extremely low NDVI values would in reality be associated with no-fire because of lack of fuel for burning. Thus, the result we obtained is just a generalization of the broad pattern where as NDVI decreases, fire occurrence increases.

Supplementary video related to this article can be found at <http://dx.doi.org/10.1016/j.apgeog.2017.05.001>

6. Conclusions

Our research shows that fires in the Colombian Caribbean result from the complex interaction of regional and local biophysical and anthropogenic factors. Fires exhibit a clear seasonal pattern related with intra and interannual rainfall variability, which in turn is related to the movement of the ITCZ and lower frequency climatic oscillations, i.e. TNA. Fires also have a distinct spatial pattern that is explained by the distribution of temperature and dry season rainfall, distance variables, and NDVI. We hypothesize that the extensive land cover transformation in this region, mostly from lowland dry forest to pasture, has led to an increase in fire activity associated with warmer and drier conditions, and to land use practices associated with cattle ranching and agriculture. Although most of the lowlands have already been cleared, this trend is likely to continue in the wetter and steeper slopes of the SNSM, Perijá and northern Andean foothills, where recent estimates show that between 1990 and 2005, ~754,000 ha of forest were cleared (Armenteras, Cabrera, Rodríguez, & Retana, 2013). As such, the extent of burned area and fire carbon emissions from the Colombian Caribbean will continue to increase.

Acknowledgments

This research was partially funded by a grant from the Inter-American Institute for Global Change Research (IAI) CRN3038, which is supported by the US National Science Foundation (Grant GEO-1128040), by an internal grant from Universidad del Norte as part of its Strategic Area in Biodiversity, Ecosystem Services and Human Well-being, and by Colciencias grant 121566044585 "Causas y consecuencias de la aridificación de ecosistemas húmedos tropicales. Una mirada climática y geológica durante el Neogeno de

Suramérica". We would like to thank two anonymous reviewers for their constructive comments.

References

- Akaike, H. (1974). A new look at the statistical model identification. In *IEEE transactions on automatic control, AC-19* (pp. 716–723).
- Amante, C., & Eakins, B. W. (2009). ETOPO1 1 arc-minute global relief Model: Procedures, data sources and analysis. In *NOAA technical memorandum NESDIS NGDC-24*. National Geophysical Data Center, NOAA.
- Armenteras, D., Cabrera, E., Rodríguez, N., & Retana, J. (2013). National and regional determinants of tropical deforestation in Colombia. *Regional Environmental Change*, 13(6), 1181–1193.
- Armenteras, D., González-Alonso, F., & Franco, C. (2009). Distribución geográfica y temporal de incendios en Colombia utilizando datos de anomalías térmicas. *Caldasia*, 31(2), 303–318.
- Armenteras, D., & Retana, J. (2012). Dynamics, patterns and causes of fires in northwestern Amazonia. *PLoS ONE*, 7(4).
- Armenteras, D., Retana, J., Molowny, R., Roman, R. M., Gonzalez, F., & Morales, M. (2011). Characterising fire spatial pattern interactions with climate and vegetation in Colombia. *Agricultural and Forest Meteorology*, 151, 279–289.
- Armenteras, D., Romero, M., & Galindo, G. (2005). Vegetation fire in the savannas of the llanos orientales of Colombia. *World Resource Review*, 17(4), 531–543.
- Bernal, G., Poveda, G., Roldán, P., & Andrade, C. (2006). Patrones de variabilidad de las temperaturas superficiales del mar en la costa Caribe colombiana. *Revista de la Academia Colombiana de Ciencias Exactas, Físicas y Naturales*, 30(115), 195–208.
- Borrelli, P., Armenteras, D., Panagos, P., Modugno, S., & Shütt, B. (2015). The implications of fire management in the andean paramo: A preliminary assessment using satellite remote sensing. *Remote Sensing*, 7, 11061–11082.
- Bowman, D. M. J. S., Balch, J. K., Artaxo, P., Bond, W. J., Carlson, J. M., Cochrane, M. A., et al. (2009). Fire in the earth system. *Science*, 481–484.
- Calderón, S. L., Romero, G., & Alterio, H. (2015). *Informe sobre los costos económicos del fenómeno de El Niño 2015*. Bogotá: Subdirección de Desarrollo Ambiental Sostenible, Departamento Nacional de Planeación.
- Cardona, A., Valencia, V. A., Bayona, G., Duque, J., Ducea, M., Gehrels, G., et al. (2011). Early-subduction-related orogeny in the northern Andes: Turonian to eocene magmatic and provenance record in the Santa Marta massif and rancheria basin, northern Colombia. *Terra Nova*, 23(1), 26–34.
- Chuvieco, E., Giglio, L., & Justice, C. (2008a). Global characterization of fire activity: Toward defining fire regimes from earth observation data. *Global Change Biology*, 14, 1488–1502.
- Chuvieco, E., Opazo, S., Sione, W., Valle, H. d., Anaya, J., Bella, C. D., et al. (2008b). Global burned-land estimation in Latin America using MODIS composite data. *Ecological Applications*, 18(1), 64–79.
- Cochrane, M. A., Alencar, A., Schulze, M. D., Souza, C. M., Nepstad, D. C., Lefebvre, P., et al. (1999). Positive feedbacks in the fire dynamic of closed canopy tropical forests. *Science*, 284(5421), 1832–1835.
- El Tiempo. (2016). *Fenómeno del Niño podría llegar hasta marzo del 2016* (In El Tiempo, Bogotá).
- Enfield, D. B., & Alfaro, E. J. (1999). The dependence of Caribbean rainfall on the interaction of the tropical Atlantic and Pacific oceans. *American Meteorological Society*, 12, 2093–2103.
- ESRI. (2014). *ArcGIS Desktop: Release 10*. Redlands: Environmental Systems Research Institute.
- Etter, A., McAlpine, C., & Possingham, H. (2008). Historical patterns and drivers of landscape change in Colombia since 1500: A regionalized spatial approach. *Annals of the Association of American Geographers*, 98(1), 2–23.
- García, H., Corzo, G., Isaacs, P., & Etter, A. (2014). Distribución y estado actual de los remanentes del bioma de bosque seco tropical en Colombia: Insumos para su gestión. In C. Pizano, & H. García (Eds.), *El bosque seco tropical en Colombia* (pp. 229–251). Bogotá: Instituto de Investigación de Recursos Biológicos Alexander von Humboldt (IAVH).
- Giglio, L. (2013). *MODIS Collection 5 active fire product user's guide, version 2.5* (p. 61). Department of Geographical Sciences, University of Maryland.
- Giglio, L., Descloitres, J., Justice, C. O., & Kaufman, Y. J. (2003). An enhanced contextual fire detection algorithm for MODIS. *Remote Sensing of Environment*, 87(2–3), 273–282.
- Giglio, L., Randerson, J. T., van der Werf, G. R., Kasibhatla, P. S., Collatz, G. J., Morton, D. C., et al. (2010). Assessing variability and long-term trends in burned area by merging multiple satellite fire products. *Biogeosciences*, 7, 1171–1186.
- Guzmán, G., Gómez, E., & Serrano, B. E. (2004). Geología de los cinturones del Sinú, San Jacinto y borde occidental del valle inferior del Magdalena, Caribe colombiano. In *Ingeominas* (p. 134). Bogotá: Ingeominas.
- Hijmans, R. J., Cameron, S. E., Parra, J. L., Jones, P. G., & Jarvis, A. (2005). Very high resolution interpolated climate surfaces for global land areas. *International Journal of Climatology*, 25, 1965–1978.
- Hintze, J. L. (2013). *NCS9 9*. In *Kaysville*.
- Hoffmann, W. A., Schroeder, W., & Jackson, R. B. (2003). Regional feedbacks among fire, climate, and tropical deforestation. *Journal of Geophysical Research*, 108(D23).
- IDEAM. (2015). *Atlas climatológico de Colombia* (vol. 2016) (Bogotá).
- Jaramillo, U., Cortés-Duque, J., & Flórez, C. (2015). *Colombia anfibia. Un país de*

- humedales. Bogotá: Instituto Alexander von Humboldt.
- Kitzberger, T., Swetnam, T. W., & Veblen, T. T. (2001). Inter-hemispheric synchrony of forest fires and the el nino-southern oscillation. *Global Ecology and Biogeography*, 10(3), 315–326.
- Kovacs, K., Ranson, K. J., Sun, G., & Kharuk, V. I. (2004). The relationship of the Terra MODIS fire product and anthropogenic features in the Central Siberian Landscape. *Earth Interactions*, 8, 1–25.
- Langenfels, R. L., Francey, R. J., Pak, B. C., Steele, L. P., Lloyd, J., Trudinger, C. M., et al. (2002). Interannual growth rate variations of atmospheric CO₂ and its $\delta^{13}\text{C}$, H₂, CH₄, and CO between 1992 and 1999 linked to biomass burning. *Global Biogeochemical Cycles*, 16(3), 21–21–21–22.
- Legendre, P., & Legendre, L. (1998). *Numerical ecology*. Oxford: Elsevier Scientific.
- Levine, N. (2013). *CrimeStat IV: A spatial statistics program for the analysis of crime incident locations (version 4.0). User manual*. Houston, Washington: Ned Levine & Associates, National Institute of Justice.
- Levine, N. (2015). *CrimeStat: A spatial statistics program for the analysis of crime incident locations (version 4.02). User manual*. Houston, Washington: Ned Levine & Associates, National Institute of Justice.
- Lima, A., Silva, T. S. F., Aragão, L. E. O. e. C. d., Feitas, R. M. d., Adami, M., Formaggio, A. R., et al. (2012). Land use and land cover changes determine the spatial relationship between fire and deforestation in the Brazilian Amazon. *Applied Geography*, 34, 239–246.
- MADS, IDEAM, IAvH, INVEMAR, IAP, SINCHI, et al. (2015). *Mapa de ecosistemas continentales, costeros y marinos de Colombia version 1.0*. In Bogotá.
- Mélice, J., & Servain, J. (2003). The tropical Atlantic meridional SST gradient index and its relationships with the SOI, NAO and Southern Ocean. *Climate Dynamics*, 20(5), 447–464.
- Mesa, O., Poveda, G., & Carvajal, L. F. (1997). *Introducción al clima de Colombia, Medellín*.
- Montes, C., Guzman, G., Bayona, G., Cardona, A., Valencia, V., & Jaramillo, C. (2010). Clockwise rotation of the Santa Marta massif and simultaneous Paleogene to neogene deformation of the plato-san jorge and cesar-ranchería basins. *Journal of South American Earth Sciences*, 29(4), 832–848.
- Ocampo, G. I. (2007). *La instauración de la ganadería en el valle del Sinú: la hacienda Marta Magdalena, 1881–1956, Medellín*.
- Oliveira, S., Pereira, J. M. C., San-Miguel-Ayanz, J., & Lourenço, L. (2014). Exploring the spatial patterns of fire density in southern europe using geographically weighted regression. *Applied Geography*, 51, 143–157.
- Parsons, J. J. (1952). The settlement of the sinu valley of Colombia. *Geographical Review*, 42(1), 67–86.
- Parsons, J. J., & Bowen, W. A. (1966). Ancient ridged fields of the san jorge river floodplain, Colombia. *Geographical Review*, 56(3), 317–343.
- Plazas, C., Falchetti, A., Sáenz, J., & Archila, S. (1993). *La sociedad hidráulica Zenú: Estudio arqueológico de 2000 años de historia en las llanuras del Caribe Colombiano. Banco de la República, Bogotá*.
- Posada-Carbó, E. (1996). *The Colombian Caribbean, a regional history 1870–1950*. Clarendon, Oxford.
- Poveda, G. (2004). La hidroclimatología de Colombia: Una síntesis desde la escala inter-decadal hasta la escala diaria. *Revista de la academia colombiana de ciencias exactas. Físicas y Naturales*, 28(107), 201–222.
- Poveda, G., Jaramillo, A., Gil, M., Quiceno, N., & Mantilla, R. (2001). Seasonality in ENSO-related precipitation, river discharges, soil moisture, and vegetation index in Colombia. *Water Resources Research*, 37(8), 2169–2178.
- Poveda, G., & Mesa, O. (2000). On the existence of Iloro (the rainiest locality on earth): Enhanced ocean-atmosphere-land interaction by a low-level jet. *Geophysical Research Letters*, 27(11), 1675–1678.
- Poveda, G., Waylen, P. R., & Pulwarty, R. S. (2006). Annual and inter-annual variability of the present climate in northern South America and southern Mesoamerica. *Palaeogeography, Palaeoclimatology, Palaeoecology*, 234(1), 3–27.
- Python Software Foundation. (2016). *Python language reference, version 2.7*.
- R Core Team. (2016). *R: A language and environment for statistical computing*. Vienna: R Foundation for Statistical Computing.
- Restrepo, J. C., Ortiz, J. C., Pierini, J., Schrottke, K., Maza, M., Otero, L., et al. (2014). Freshwater discharge into the caribbean sea from the rivers of northwestern south America (Colombia): Magnitude, variability and recent changes. *Journal of Hydrology*, 509, 266–281.
- Romero-Ruiz, M., Etter, A., Sarmiento, A., & Tansey, K. (2010). Spatial and temporal variability of fires in relation to ecosystems, land tenure and rainfall in savannas of northern South America. *Global Change Biology*, 16, 2013–2023.
- Semana. (2016). *El fenómeno de El Niño llega a su etapa final*. Bogotá: Revista Semana.
- Servicio Geológico Colombiano. (2015). *Atlas geológico de Colombia. In Bogotá*.
- Tschanz, C. M., Marvin, R. F., Cruz, B. J., Mehnert, H. H., & Cebula, G. T. (1974). Geologic evolution of the Sierra Nevada de Santa Marta, Northeastern Colombia. *Geological Society of America Bulletin*, 85(2), 273–284.
- Van Ausdal, S. (2009). *Potrerros, ganancias y poder. Una historia ambiental de la ganadería en Colombia, 1850–1950*. Historia Crítica, Special edition.
- Venables, W. N., & Ripley, B. D. (2002). *Modern applied statistics with S*. New York: Springer.
- Vilardy, S. P., González, J. A., Martín-López, B., Oteros-Rozas, E., & Montes, C. (2012). Los servicios de los ecosistemas de la Reserva de Biosfera Ciénaga Grande de Santa Marta. *Revista Iberoamericana de Economía Ecológica*, 19, 66–83.
- Weber, M., Cardona, A., Valencia, V., García-Casco, A., Tobón, M., & Zapata, S. (2010). U/Pb detrital zircon provenance from late cretaceous metamorphic units of the Guajira Peninsula, Colombia: Tectonic implications on the collision between the Caribbean arc and the South American margin. *Journal of South American Earth Sciences*, 29, 805–816.
- van der Werf, G. R., Dempewolf, J., Trigg, S. N., Randerson, J. T., Kasibhatla, P. S., Giglio, L., et al. (2008). Climate regulation of fire emissions and deforestation in equatorial Asia. *Proceedings of the National Academy of Sciences*, 105(51), 20350–20355.
- van der Werf, G. R., Randerson, J. T., Collatz, G. J., & Giglio, L. (2003). Carbon emissions from fires in tropical and subtropical ecosystems. *Global Change Biology*, 9, 547–562.
- van der Werf, G. R., Randerson, J. T., Giglio, L., Collatz, G. J., Kasibhatla, P. S., & Arellano, A. F. (2006). Interannual variability in global biomass burning emissions from 1997 to 2004. *Atmospheric Chemistry and Physics*, 6, 3423–3441.
- van der Werf, G. R., Randerson, J. T., Giglio, L., Collatz, G. J., Mu, M., Kasibhatla, P. S., et al. (2010). Global fire emissions and the contribution of deforestation, savanna, forest, agricultural, and peat fires (1997–2009). *Atmospheric Chemistry and Physics*, 10, 11707–11735.
- Zambrano, F. (2000). La historia del poblamiento del territorio de la región Caribe de Colombia. In A. Abello, & S. Giaino (Eds.), *Poblamiento y ciudades del Caribe Colombiano. Fonade*. Bogotá: Observatorio del Caribe Colombiano.